

Biomechanical comparison of locked versus non-locked symphyseal plating of unstable pelvic ring injuries

R. J. Godinsky¹ · G. A. Vrabec¹ · L. M. Guseila² · D. E. Filipkowski² · J. J. Elias² 

Received: 20 November 2015 / Accepted: 7 March 2016 / Published online: 17 March 2016
© Springer-Verlag Berlin Heidelberg 2016

Abstract

Purpose Locked symphyseal plates are utilized to provide higher levels of construct stiffness than non-locked plates. The current biomechanical study was performed to compare stiffness at the pubic symphysis between locked and non-locked plating systems.

Methods Synthetic models were utilized to represent injury to the pelvis and symphyseal plating combined with a sacro-iliac screw. Seven models were evaluated with plates and locking screws, and seven were evaluated with non-locking screws. Single limb stance was simulated, with all models loaded for 1000 cycles with 350 N applied at the sacrum. Two pairs of markers crossing the symphysis were tracked with a video-based tracking system. A coordinate system was developed to quantify motion between the pairs in three directions: medial–lateral gap, anterior–posterior shear translation, and superior–inferior shear translation. Significant differences between the plating systems were identified with *t* tests ($p < 0.05$).

Results Anterior–posterior shear translation varied significantly between the two plating systems. From cycles 100 to 1000, average shear translation for the non-locked and locked systems was ~0.7 and 0.3 mm, respectively, at the markers closest to the plate and 2.2 and 1.4 mm, respectively, at the markers further from the plate. Motion in the other two directions did not differ significantly between locked and non-locked models.

Conclusions Locked symphyseal plating systems can provide better stability than non-locked systems for anterior–posterior shear translation. More stability could potentially reduce the risk of failure of the plate or screws.

Keywords Symphyseal plating · Locked plating · Pelvis · Biomechanics

Introduction

Disruption of the pelvic ring results in complex injury patterns that often require operative intervention. Approximately, 40 % of the ring's stability comes from the anterior aspect of the ring, specifically the pubic symphysis and its ligaments [1]. Classically, disruption of the pubic symphysis has been treated via open reduction internal fixation using a symphyseal plate construct. If the posterior ring is also disrupted, screw fixation has become the standard for the sacro-iliac joint. Normal functional loading can lead to failure of symphyseal plating constructs. Failure can occur in the forms of progressive screw loosening, screw breakage, plate breakage, and in some cases catastrophic failure [2–4].

Symphyseal plating systems with locking screws are designed to reduce motion at the interface of the plate and screw, and thereby improve stability across the pubic symphysis. Although improved stability theoretically reduces the risk of failure, particularly for fracture patterns including ligamentous injury, failure modes common for non-locked plating systems have also been identified with locked plates [2]. Multiple biomechanical studies have compared non-locked to locked plating systems during simulated functional loading, without identifying any differences in stability between the two. Two previous studies

✉ J. J. Elias
john.elias@akrongeneral.org

¹ Department of Orthopaedic Surgery, Cleveland Clinic Akron General, Akron, OH, USA

² Department of Research, Cleveland Clinic Akron General, 1 Akron General Ave, Akron, OH 44307, USA

applied simulated dual limb stance, and found no differences in symphyseal opening as measured by calipers [5, 6]. One study evaluated relative rotations and translations between the two hemi-pelvises during dynamic single limb stance [7], also without finding a difference. Data comparing the plating systems based on three-dimensional measurements at the symphysis during dynamic motion are currently lacking.

The current study was performed to further characterize the influence of locked plating systems on stability at the pubic symphysis. The study focused on three-dimensional measurements of gap formation across the symphysis during cyclic motion. The hypothesis is that a locked plating system provides more stability at the pubic symphysis than a non-locked system.

Materials and methods

Injury, reconstruction and function were simulated with fourteen full male synthetic pelvis models (Sawbones model 1301-1, Vashon Island, WA), including a hard cortical shell and cancellous core [7–9]. The pelvis models were utilized to minimize variations between specimens. Without representation of soft tissues at the pubic symphysis, an anterior–posterior compression injury requiring both anterior and posterior fixation was simulated by disrupting the left sacro-iliac joint (OTA 61-C 1.2) [10]. The multiple screws and glue used by the manufacturer to secure the right sacro-iliac joint were not disturbed. A standard 3.5 mm six-hole symphyseal plate (Synthes, West Chester, PA), which can be secured with locking or non-locking screws, was utilized to stabilize the pubic symphysis for all specimens. Seven specimens were instrumented with the plate locked while the other seven were instrumented with the plate non-locked.

Prior to instrumentation, the left hemi-pelvis was reduced to the intact right hemi-pelvis and sacrum. After reduction, the left sacro-iliac joint was instrumented using a 7.3 mm partially threaded cannulated screw and washer (Synthes, West Chester, PA). All screws were inserted at the S1 level. A guide wire was placed utilizing direct visualization and fluoroscopy with appropriate positioning confirmed on both inlet and outlet radiographic views. Proper position of the guide wire was confirmed with fluoroscopy on both inlet and outlet radiographs. A cannulated drill was used to drill the near cortex. The screw was inserted with a washer and tightened to 0.9 N-m using an electronic torque limiter.

Anterior instrumentation was performed under direct visualization using six holes on the symphyseal plate. The pre-contoured symphyseal plate was positioned along the anterior pelvic ring and screw-in guides were used for

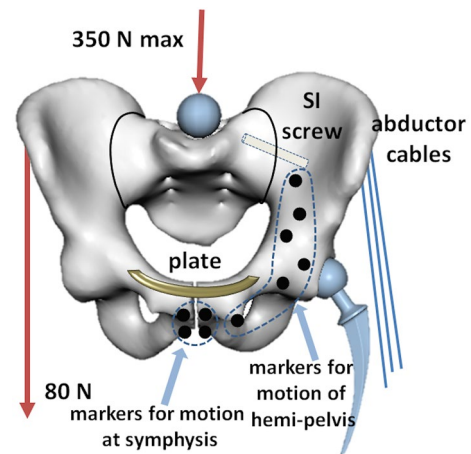


Fig. 1 Schematic diagram showing representation of single limb stance with the pelvis models. The diagram shows the maximum force applied at the sacrum during cyclic loading (350 N) and the force applied to represent the contralateral limb (80 N). The pelvis was stabilized with cables representing the abductor muscles, and markers were tracked to characterize motion of the pelvis

drilling for both locked and non-locked screw placement. Non-locked screws (3.5 mm cortical screws, Synthes, West Chester, PA) were uniformly tightened to 0.9 N-m using the torque limiter. Locked screws of the same size as the non-locked (Synthes, West Chester, PA) were hand tightened using the torque limiting screwdriver until the locked screw head was flush with the plate. Fluoroscopy was used to check the final construct and hardware position.

The stability of the symphyseal plating systems was evaluated using a cyclic loading regimen designed to simulate single limb stance (Fig. 1) [7, 11]. Single limb stance was chosen to produce greater pelvic instability than induced by dual limb stance [11]. The pelvis models were supported at the acetabulum on the side with the sacro-iliac injury by a hip stem. The hip stem was embedded in low-melting point alloy at an angle of 15° adduction to simulate single limb stance. Forces were applied at the sacrum and the unsupported hip to replicate loading from body weight superior to the pelvis and weight of the leg, respectively, during single limb stance. The force magnitudes chosen were based on the largest forces previously shown to allow for stable cyclic loading [11, 12]. A ball connector fixed to the actuator of a material testing machine (MTS, Eden Prairie, MN) was positioned in contact with the proximal sacrum to apply a vertical load with no moments transferred to the sacrum. Cyclic loading was applied between 150 and 350 N at a rate of 1 Hz to a total of 1000 cycles. At the unsupported hip, a construct of weights and pulleys applied a vertical force of 80 N to the iliac wing. Abductor muscles at the supported hip were represented with steel cables projecting from a reinforced iliac wing to points of

fixation at the base of the testing machine. The abductor cables were tightened to align the pelvis horizontally with the sacrum loaded to 150 N, with the anterior superior iliac spines aligned with the pubic tubercle in a vertical plane. Each model was visually inspected following testing.

Motion at the symphysis was measured with a video tracking system (MaxTRAQ 3D, Innovision Systems, Columbiaville, MI). Three cameras calibrated by a standardized frame were used to record the motion of black spherical pinheads (markers) inserted into the models at a rate of 30 Hz. The markers were positioned in two pairs crossing the symphysis, with additional markers distributed along the pelvis to monitor motion of the entire construct (Fig. 1). Software for the motion tracking system was used to quantify the position of each marker in three dimensions. The spatial resolution of the system is in the order of 0.1 mm [13].

The marker data were read into custom written software (Matlab, Mathworks, Natick, MA) for characterizing the motion at each pair of markers crossing the symphysis. With the pelvis unloaded, a local coordinate system was created at the symphysis (Fig. 2). The local coordinate system included an axis connecting the pair of markers crossing the symphysis closest to the plate. A second axis was perpendicular to the first axis and an axis between two markers along the symphysis on the side supported by the hip stem. The third axis was perpendicular to the other two. The third axis represented a normal to the plane of the symphysis, represented by the four markers at the symphysis. These axes allowed measurements of the change in the distances between pairs of markers crossing the symphysis for medial–lateral (ML) gap, superior–inferior (SI) shear translation (as observed on an outlet view of the pelvis), and anterior–posterior (AP) shear translation (as observed on an inlet view). Repeated measurements as the position of a pelvis model was varied showed repeatability of less than 0.1 mm for distances between markers in all directions. To maintain the orientations of these axes with respect to the

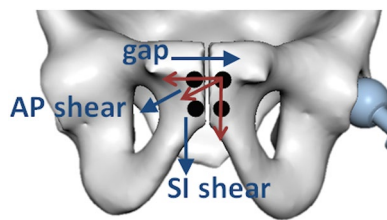


Fig. 2 Schematic diagram showing the markers at the symphysis and axes for the coordinate system fixed to the supported hemi-pelvis. Directions for gap closing, anterior–posterior (AP) shear translation, and superior–inferior (SI) shear translation of the unsupported hemi-pelvis with respect to the coordinate system are also shown. The field of view has been rotated to be in line with an outlet view of the pelvis rather than the AP view of the pelvis as oriented for testing

symphysis, the coordinate system translated and rotated with the supported hemi-pelvis based on the motion of six markers distributed along the hemi-pelvis. Translations and rotations for aligning the position of markers on the hemi-pelvis in the unloaded position to each loaded position were quantified using an iterative closest point algorithm [14]. The translations and rotations were applied to the coordinate axes to maintain the orientation with respect to the supported hemi-pelvis at each loaded position.

The marker data were captured with each specimen unloaded and for three successive cycles at the initiation of cyclic loading and at 100 cycle intervals. At cycle 1 and at cycle 800, marker data from one specimen in the locked group could not be processed due to poor resolution of a marker from the motion tracking system. The position of each marker along each axis as a function of time during cyclic loading was processed through a Gaussian filter for smoothing. At each interval of cyclic motion, distances between the pairs of markers closest to the plate (top) and furthest from the plate (bottom) were quantified in all three directions and averaged over the three successive cycles. Changes in distances between pairs from the unloaded condition were quantified at each interval of cyclic motion and compared between the locked and non-locked conditions with *t* tests after verifying that the data were normally distributed with an Anderson–Darling test. The level of statistical significance was set at $p < 0.05$.

Results

Variation in the distance between markers primarily occurred for AP shear translation. For the models with non-locked screws, the AP shear translation of the unsupported hemi-pelvis with respect to the supported side tended to increase from cycle 1 to 100, and hold steady until 1000 cycles (Table 1). The locked models showed minimal change during cyclic loading. For the top markers, the average (\pm standard deviation) translation at 1000 cycles was 0.7 ± 0.2 mm for the non-locked models, compared to 0.3 ± 0.2 mm for the locked models (57 % decrease). For the bottom markers the average translation at 1000 cycles was 2.3 ± 0.6 mm for the non-locked models, compared to 1.4 ± 0.6 mm for the locked models (39 % decrease). Similar changes were noted from 100 to 900 cycles, with significant differences ($p < 0.05$) noted for nearly all comparisons beyond cycle 1.

For ML gap (Table 2) and SI shear translation (Table 3) the changes in distance between markers were smaller than those measured for AP shear translation with minimal variation from 1 to 1000 cycles. The average ML gap closing was less than 0.1 mm at the top markers and ~ 1.0 mm at the bottom markers throughout cyclic loading.

Table 1 Average (\pm standard deviation) anterior–posterior shear translation at the symphysis (mm)

Cycle	Top markers			Bottom markers		
	Locked	Non-locked	<i>P</i> value	Locked	Non-locked	<i>P</i> value
1	0.3 \pm 0.2	0.5 \pm 0.2	0.15	1.2 \pm 0.5	1.6 \pm 0.5	0.18
100	0.3 \pm 0.2	0.7 \pm 0.2	0.02	1.3 \pm 0.5	2.0 \pm 0.6	0.04
200	0.4 \pm 0.3	0.7 \pm 0.2	0.04	1.4 \pm 0.6	2.1 \pm 0.6	0.06
300	0.4 \pm 0.3	0.7 \pm 0.2	0.08	1.4 \pm 0.6	2.1 \pm 0.6	0.05
400	0.4 \pm 0.2	0.7 \pm 0.3	0.04	1.4 \pm 0.6	2.1 \pm 0.6	0.03
500	0.3 \pm 0.2	0.7 \pm 0.2	0.01	1.4 \pm 0.6	2.1 \pm 0.6	0.04
600	0.3 \pm 0.2	0.8 \pm 0.3	0.01	1.3 \pm 0.6	2.2 \pm 0.6	0.02
700	0.4 \pm 0.2	0.7 \pm 0.2	0.01	1.3 \pm 0.6	2.2 \pm 0.6	0.02
800	0.3 \pm 0.2	0.7 \pm 0.2	0.01	1.3 \pm 0.6	2.2 \pm 0.6	0.02
900	0.3 \pm 0.2	0.7 \pm 0.2	0.02	1.3 \pm 0.6	2.2 \pm 0.6	0.01
1000	0.3 \pm 0.2	0.7 \pm 0.2	0.01	1.4 \pm 0.6	2.3 \pm 0.6	0.02

Table 2 Average (\pm standard deviation) medial–lateral gap closing at the symphysis (mm)

Cycle	Top markers			Bottom markers		
	Locked	Non-locked	<i>P</i> value	Locked	Non-locked	<i>P</i> value
1	0.06 \pm 0.2	0.06 \pm 0.2	0.9	0.8 \pm 1.0	1.0 \pm 0.8	0.8
100	0.05 \pm 0.2	0.06 \pm 0.2	0.9	0.9 \pm 1.0	1.1 \pm 0.9	0.7
200	0.001 \pm 0.2	0.07 \pm 0.2	0.6	0.9 \pm 0.9	1.1 \pm 1.0	0.7
300	0.08 \pm 0.2	0.07 \pm 0.2	0.9	0.9 \pm 0.9	1.1 \pm 1.0	0.7
400	0.06 \pm 0.2	0.05 \pm 0.3	0.9	0.9 \pm 1.0	1.1 \pm 1.0	0.7
500	0.06 \pm 0.2	0.05 \pm 0.2	0.9	0.9 \pm 1.0	1.1 \pm 1.0	0.7
600	0.06 \pm 0.2	0.05 \pm 0.3	0.9	0.9 \pm 1.0	1.1 \pm 1.0	0.7
700	0.05 \pm 0.2	0.07 \pm 0.2	0.9	0.9 \pm 1.0	1.1 \pm 1.0	0.7
800	0.09 \pm 0.2	0.06 \pm 0.2	0.8	1.0 \pm 1.0	1.1 \pm 1.0	0.9
900	0.06 \pm 0.2	0.06 \pm 0.2	0.9	0.9 \pm 1.0	1.1 \pm 1.0	0.7
1000	0.03 \pm 0.2	0.06 \pm 0.2	0.9	0.9 \pm 1.0	1.1 \pm 1.0	0.7

Table 3 Average (\pm standard deviation) superior–inferior shear translation at the symphysis (mm)

Cycle	Top markers			Bottom markers		
	Locked	Non-locked	<i>P</i> value	Locked	Non-locked	<i>P</i> value
1	0.01 \pm 0.2	−0.02 \pm 0.3	0.8	0.1 \pm 0.4	−0.06 \pm 0.8	0.8
100	0.02 \pm 0.3	0.02 \pm 0.2	0.9	0.1 \pm 0.4	0.06 \pm 0.9	0.7
200	0.3 \pm 0.8	0.05 \pm 0.3	0.5	0.2 \pm 0.6	0.04 \pm 1.0	0.7
300	0.2 \pm 0.6	0.02 \pm 0.3	0.5	0.2 \pm 0.6	0.03 \pm 1.0	0.7
400	0.06 \pm 0.3	0.04 \pm 0.3	0.9	0.2 \pm 0.4	0.04 \pm 1.0	0.7
500	0.04 \pm 0.3	0.05 \pm 0.3	0.9	0.1 \pm 0.3	0.04 \pm 1.0	0.7
600	0.01 \pm 0.3	0.1 \pm 0.2	0.5	0.1 \pm 0.4	0.07 \pm 1.0	0.7
700	0.09 \pm 0.3	0.05 \pm 0.3	0.8	0.1 \pm 0.4	0.06 \pm 1.0	0.7
800	−0.08 \pm 0.2	0.05 \pm 0.3	0.4	0.02 \pm 0.4	0.05 \pm 1.0	0.9
900	−0.002 \pm 0.2	−0.01 \pm 0.3	0.9	0.05 \pm 0.4	0.05 \pm 1.0	0.7
1000	−0.03 \pm 0.2	0.04 \pm 0.3	0.6	0.1 \pm 0.4	0.08 \pm 1.0	0.7

Average SI shear translation was 0.3 mm or smaller for all loading cycles. No significant differences were identified between the locked and non-locked conditions for

either ML gap closing or SI shear translation ($p \geq 0.4$). No gross screw motion was observed for any model following testing.

Discussion

The results of the current study indicate that locked plating of the pubic symphysis results in a more stable construct than non-locked plating in unilateral, unstable, AP pelvic compression injuries (OTA 61-C 1.2). The increased stability was measured with respect to AP shear translation. This translation of the unsupported hemi-pelvis with respect to the supported hemi-pelvis was due to the reaction force at the acetabulum supporting only one hemi-pelvis as the sacrum was physiologically oriented and loaded vertically to represent single limb stance. The AP translation was larger than ML gap closure or SI shear translation. Adjacent to the plate, using the locked screws decreased average AP translation by more than 50 % as compared to the non-locked screws.

Previous biomechanical studies have not identified a difference in construct stiffness between locked and non-locked plating systems, with the testing methods likely contributing to a different result for the current study. Two previous cadaveric studies found no differences between the plating systems based on static measures of ML gap opening at the symphysis following application of 1 million cycles of simulated dual limb stance [5, 6]. Another study found no differences between the plating systems while quantifying relative translations and rotations between the two hemi-pelves while representing dynamic single limb stance with uniform pelvis models [7]. Similar to the dynamic study, the current study simulated the asymmetric loading pattern of single limb stance to produce greater pelvic instability than dual limb stance [11] and tested synthetic pelvis models to minimize variations between specimens. The current study applied larger loads during dynamic representation of single limb stance than the previous study (350 N vs. 150 N at the sacrum and 80 N vs. 0 N at the contralateral hip) and characterized motion in three dimensions within a coordinate system positioned at the symphysis. The axes of the coordinate system were reoriented based on motion of the supported hemi-pelvis to maintain a consistent orientation with respect to the moving symphysis throughout cyclic motion. The efforts to minimize variations between specimens, maximize measurement accuracy, and aggressively load the models likely contributed to identification of the small difference in AP shear translation between the two plating systems.

Reduced motion at the symphysis with locked plates potentially provides a clinical benefit. Although the enhanced construct stiffness with locked plates occurred for only AP shear translation, and the motion decreased by less than 1 mm, the relative change where the largest motion occurred was 39 %. Differences in motion between locked and non-locked plates could be larger for more demanding

loading conditions, such as walking. The current loading conditions were limited to representation of single limb stance to ensure stability of the models representing the hip throughout cyclic loading. The primary concern for the pelvic trauma simulated is typically ML gap opening. The current study focused on single limb stance that induces gap closing [11] due to the previous studies identifying no differences in gap opening between the plating systems with dual limb stance [5, 6]. Based on the current results, reexamination of gap opening with uniform models and dynamic tracking of gap formation may be warranted. The increased stability that was noted for the locked plating systems could reduce the risk of failure modes noted for non-locked plates, such as screw loosening and failure and plate failure [3, 4], although failure due to conditions such as screw loosening and failure have also been noted for locked plating systems [2, 15]. Increased construct stiffness could potentially allow for earlier mobility following treatment. Ligamentous and soft tissue healing could also be enhanced by the increase in construct stiffness. With prolonged time to heal injury patterns including soft tissue/ligamentous injury, increased construct stiffness would theoretically improve short- and long-term maintenance of reduction and ultimate healing.

While the synthetic pelvis models provided specimen uniformity, they can also be considered a limitation of the study, due to differences in properties with respect to the *in vivo* condition. These models have been used for multiple previous biomechanical studies focused on stabilizing the pelvis, including measures of motion and/or plating at the symphysis [7–9]. The models produced stable motion patterns for force levels previously applied to embalmed cadaveric specimens to represent single limb stance [11, 12]. The limit of 1000 loading cycles was set due to the minimal variation in distances between markers crossing the symphysis beyond 100 cycles for both plating systems, rather than a concern for integrity of the models.

Conclusion

Locked plating systems can provide better construct stability than non-locked systems for OTA 61-C 1.2 injuries. In particular, the improved stability is related to AP shear translation. Although the magnitude of the translation noted for the current study is relatively small, the potential benefit for *in vivo* loading conditions should be considered. Improved stability could potentially reduce the risk of failure due to screw loosening or failure of a screw or plate.

Acknowledgments Funding and materials for the study were provided by DePuy Synthes.

Compliance with ethical requirements

Conflict of interest Gregory Vrabec received a research grant and materials from DePuy Synthes to conduct the study. Ryan Godinsky, Loredana Guseila, Danielle Filipkowski, and John Elias declare no conflict of interest.

References

1. Tile M, Hearn T, Vrahas M. Biomechanics of the pelvic ring. In: Tile M, Helfet DL, Kellam JF, editors. *Fractures of the pelvis and acetabulum*. 3rd ed. Philadelphia: Lippincott Williams & Wilkins; 2003. p. 32–45.
2. Moed BR, Grimshaw CS, Segina DN. Failure of locked design-specific plate fixation of the pubic symphysis: a report of six cases. *J Orthop Trauma*. 2012;26:e71–5.
3. Putnis SE, Pearce R, Wali UJ, Bircher MD, Rickman MS. Open reduction and internal fixation of a traumatic diastasis of the pubic symphysis: one-year radiological and functional outcomes. *J Bone Joint Surg Br*. 2011;93:78–84.
4. Sagi HC, Papp S. Comparative radiographic and clinical outcome of two-hole and multi-hole symphyseal plating. *J Orthop Trauma*. 2008;22:373–8.
5. Grimshaw CS, Bledsoe JG, Moed BR. Locked versus standard unlocked plating of the pubic symphysis: a cadaver biomechanical study. *J Orthop Trauma*. 2012;26:402–6.
6. Moed BR, O'Boynick CP, Bledsoe JG. Locked versus standard unlocked plating of the symphysis pubis in a Type-C pelvic injury: a cadaver biomechanical study. *Injury*. 2014;45:748–51.
7. Prasarn ML, Zych G, Gaski G, Baria D, Kaimrajh D, Milne T, Latta LL. Biomechanical study of 4-hole pubic symphyseal plating: locked versus unlocked constructs. *Orthopedics*. 2012;35:e1028–32.
8. Berber O, Amis AA, Day AC. Biomechanical testing of a concept of posterior pelvic reconstruction in rotationally and vertically unstable fractures. *J Bone Joint Surg Br*. 2011;93:237–44.
9. Yinger K, Scalise J, Olson SA, Bay BK, Finkemeier CG. Biomechanical comparison of posterior pelvic ring fixation. *J Orthop Trauma*. 2003;17:481–7.
10. Marsh JL, Slongo TF, Agel J, Broderick JS, Creevey W, DeCoster TA, Prokuski L, Sirkin MS, Ziran B, Henley B, Audigé L. *Fracture and Dislocation Classification Compendium—2007: Orthopaedic Trauma Association Classification, Database and Outcomes Committee*. *J Orthop Trauma*. 2007;21(10 Suppl):S1–133.
11. MacAvoy MC, McClellan RT, Goodman SB, Chien CR, Allen WA, van der Meulen MC. Stability of open-book pelvic fractures using a new biomechanical model of single-limb stance. *J Orthop Trauma*. 1997;11:590–3.
12. Schildhauer TA, Ledoux WR, Chapman JR, Henley MB, Tencer AF, Routt ML Jr. Triangular osteosynthesis and iliosacral screw fixation for unstable sacral fractures: a cadaveric and biomechanical evaluation under cyclic loads. *J Orthop Trauma*. 2003;17:22–31.
13. Burkhart SS, Denard PJ, Konicek J, Hanypsiak BT. Biomechanical validation of load-sharing rip-stop fixation for the repair of tissue-deficient rotator cuff tears. *Am J Sports Med*. 2014;42:457–62.
14. Besl PJ, McKay ND. A method for registration of 3-D shapes. *IEEE Trans Pattern Anal Mach Intel*. 1992;14:239–56.
15. Hamad A, Pavlou G, Dwyer J, Lim J. Management of pubic symphysis diastasis with locking plates: a report of 11 cases. *Injury*. 2013;44:947–51.